TU/e EINDHOVEN UNIVERSITY OF TECHNOLOGY

Foot placement indicator for balance of planar bipeds with point feet

Citation for published version (APA):
Zutven, van, P. W. M., & Nijmeijer, H. (2013). Foot placement indicator for balance of planar bipeds with point feet. *International Journal of Advanced Robotic Systems*, *10*, 1-11. https://doi.org/10.5772/56523

DOI:
10.5772/56523

Document status and date:
Published: 01/01/2013

Document Version:
Publisher's PDF, also known as Version of Record (includes final page, issue and volume numbers)

Please check the document version of this publication:

• A submitted manuscript is the version of the article upon submission and before peer-review. There can be important differences between the submitted version and the official published version of record. People interested in the research are advised to contact the author for the final version of the publication, or visit the DOI to the publisher's website.
• The final author version and the galley proof are versions of the publication after peer review.
• The final published version features the final layout of the paper including the volume, issue and page numbers.

Link to publication

General rights
Copyright and moral rights for the publications made accessible in the public portal are retained by the authors and/or other copyright owners and it is a condition of accessing publications that users recognise and abide by the legal requirements associated with these rights.

• Users may download and print one copy of any publication from the public portal for the purpose of private study or research.
• You may not further distribute the material or use it for any profit-making activity or commercial gain
• You may freely distribute the URL identifying the publication in the public portal.

If the publication is distributed under the terms of Article 25fa of the Dutch Copyright Act, indicated by the "Taverne" license above, please follow below link for the End User Agreement:

www.tue.nl/taverne

Take down policy
If you believe that this document breaches copyright please contact us at:

openaccess@tue.nl

providing details and we will investigate your claim.

Download date: 17. Nov. 2023

INTECH
open science | open minds

International Journal of Advanced Robotic Systems

OPEN ACCESS
ARTICLE

Foot Placement Indicator for Balance of Planar Bipeds with Point Feet

Regular Paper

Pieter van Zutven[1,*] and Henk Nijmeijer[1]

1 Dynamics and Control Group, Department of Mechanical Engineering, Eindhoven University of Technology, Eindhoven, the Netherlands
* Corresponding author E-mail: p.w.m.v.zutven@tue.nl

Received 22 Aug 2012; Accepted 9 Apr 2013

DOI: 10.5772/56523

© 2013 van Zutven and Nijmeijer; licensee InTech. This is an open access article distributed under the terms of the Creative Commons Attribution License (http://creativecommons.org/licenses/by/3.0), which permits unrestricted use, distribution, and reproduction in any medium, provided the original work is properly cited.

Abstract If humanoid robots are to be used in society, they should be able to maintain their balance. Knowing where to step is crucially important. In this paper we contribute an algorithm that can compute the foot step location such that bipedal balance is maintained for planar bipeds with point feet and an arbitrary number of non-massless links on a horizontal and flat ground. The algorithm is called the foot placement indicator (FPI) and it extends the foot placement estimator (FPE). The FPE uses an inverted pendulum model to capture the dynamics of a humanoid robot, whereas the FPI deals with multi-body models with distributed masses. This paper analyses equilibrium sets and the stability of planar bipeds with point feet. The algorithm uses conservation of energy throughout the step, taking into account the instantaneous impact dynamics at foot strike. A simulation case study on a five-link planar biped shows the effectiveness of the FPI.

Keywords Humanoid Robots, Bipedal Balance, Foot Placement

1. Introduction

Many strategies for the balance of humanoid robots have been proposed in recent years. Although these strategies show promising experimental results in labs, a general breakthrough for humanoid robots in society is still far away. The main problem that current humanoid robots face before they can be deployed in society is the lack of robustness in locomotion [1]. Robustness is a measure for how well the biped performs against unforeseen disturbances such as pushes. Often these disturbances need to be suppressed by an active controller. Notable controllers that have been proposed in the past include, but are not limited to: virtual model control [2], controlled symmetries [3], inverted pendulum control [4], capture point (CP) [5] and the foot placement estimator (FPE) [6]. The stability of such control strategies is mostly analysed through Poincaré return maps [7-10], angular momentum [11, 12] or hybrid zero dynamics [10], making use of several balance criteria for humanoid robots such as the zero moment point (ZMP) [13], foot rotation indicator (FRI) [14], centroidal moment pivot (CMP) [15, 16] and capturability region [17, 18]. These criteria for balance can rigorously be divided into two groups.

First, there are criteria that consider the orientation of the stance foot with respect to the ground as a measure for balance. Indeed, as long as the stance foot of the biped does not tip over, the biped remains fully actuated and we can guarantee that it will not fall. However, these

strategies are rather conservative [19], because to maintain the balance it is not necessary that the stance foot does not tip over. Humans are the perfect counterexample, since we normally tip our stance foot during walking. Moreover, to improve robustness of humanoid robots, we must also analyse tipping of the stance foot, since these situations definitely occur when operating in a societal environment.

The second group of criteria considers proper foot placement for balance. Indeed, we maintain our balance if we know where to put our swing foot in order not to fall. So knowing where to step is crucial for the balance of a biped and may lead to increased robustness. Due to the importance of proper foot placement, we focus on foot placement strategies in this paper. Strategies that compute where to step in order to keep the balance include CP [5] and the FPE [6]. Both strategies use energy conservation of a very simple (linear) inverted pendulum model to determine where to step. It is arguable whether a complex biped with non-massless legs, torso and arms can be cast into this framework [10, 26]. The kinetic and potential energy of the biped depend on the configuration of its legs, torso and arms. Moreover, the model used in the CP method does not include any impact dynamics. In our opinion, the instantaneous swapping of the stance and swing leg in these simple models without a double support phase, does influence the energy contained in the system. Therefore, we believe that more complex models and strategies that take into account the full dynamics of the biped including ground impact are needed to compute proper foot placement.

In this paper we contribute an extension of the FPE method to compute where a biped needs to step in order to maintain its balance. We will refer to this extension as the foot placement indicator (FPI) [20]. The FPI algorithm uses conservation of energy throughout the step. It works for planar bipeds with point feet and an arbitrary number of non-massless links on a horizontal and flat ground. Unlike (linear) inverted pendulum methods that are used in the FPE and CP methods, this algorithm takes into account impact dynamics and the energy of all links of the biped to determine proper foot placement. In the extension of the FPE algorithm, ultimately resulting in the FPI algorithm, we contribute a thorough mathematical analysis of the equilibrium sets and stability of the model of the planar biped with point feet. Finally, we apply the algorithm in simulation to a five-link planar biped and show that we can accurately compute the point where the biped needs to step in order to maintain its balance.

This paper is organized as follows. In Section 2 we introduce a general model for planar bipeds with point feet and give a thorough mathematical analysis of its equilibrium sets and stability for the case where it is controlled in a rigid posture. This analysis is used in Section 3 to extend the FPE algorithm from an inverted pendulum model to the FPI algorithm that is able to balance a planar biped with distributed masses by proper foot placement. In Section 4 we evaluate results in a simulation of a five-link biped robot. The paper ends with conclusions and suggestions for future research.

2. Planar Bipeds with Point Feet

We first introduce a general model for planar bipeds with point feet on a horizontal and flat ground, after which we mathematically analyse the equilibrium sets and stability of this model when it is controlled in a rigid posture.

2.1 General Model

Under the following assumptions we can model the planar biped with point feet as a chain of rigid bodies from stance foot to swing foot:

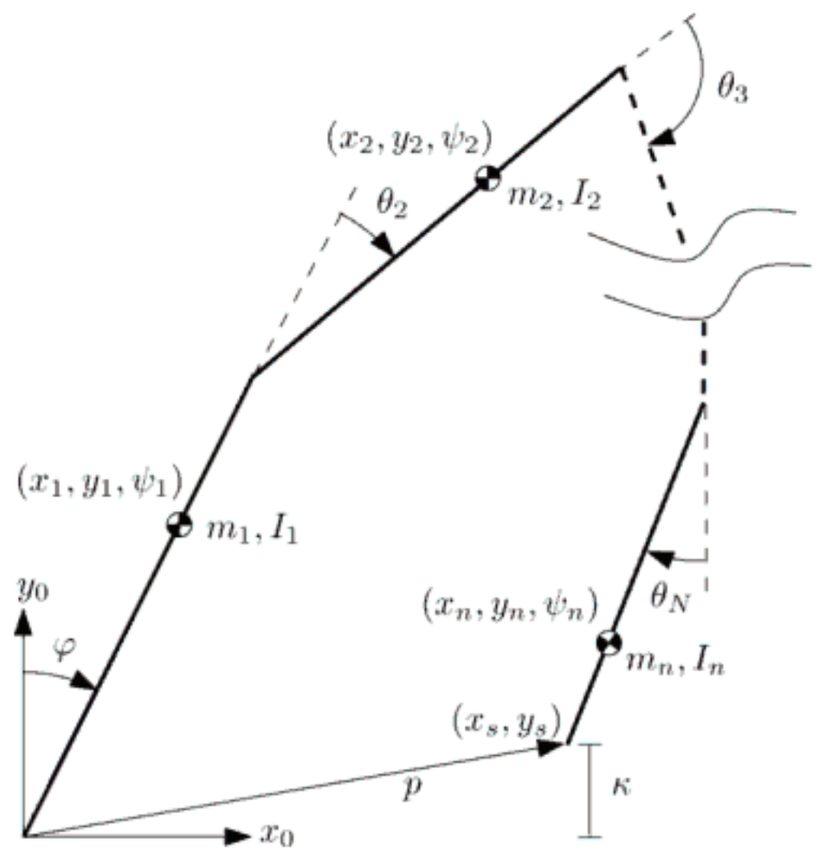

Figure 1. Schematic of a general model of a planar biped with point feet

- No slippage occurs between the stance foot and the ground, so the biped is pin-pointed to the ground in the stance foot. Here the base coordinate frame is placed. The ground is horizontal and flat.
- The biped consists of N links and n point masses m_i and moments of inertia I_i, $i = 1, \ldots, n$. The biped has $N-1$ independently actuated revolute joints described by the relative coordinates θ_j, $j = 2, \ldots, N$ and one non-actuated revolute joint described by the absolute coordinate φ, representing the absolute angle between the first link and the ground. The horizontal and vertical positions and orientation of each mass m_i with respect to the base frame are represented by x_i, y_i and ψ_i respectively.
- Impact occurs if the swing leg end comes into contact with the ground. The impact is instantaneous, so external forces are represented by impulses, actuators are ignored during the impact for standard reasons [21], and the impact results in an

instantaneous change of the velocity but no change in configuration. At the moment of impact, the swing and stance legs swap their roles, so the stance foot lifts from the ground and the swing foot stays on the ground without slipping or rebounding.

Taking into account these assumptions, the biped model can be written as an impulsive system [10] pp. 45-79:

$$\Sigma = \begin{cases} \dot{x}(t) = f(x) + g(x)u, & x \in \mathcal{S} \quad \text{a} \\ x_+ = d(x_-), & x \notin \mathcal{S} \quad \text{b} \end{cases} \tag{1}$$

with

$$f(x) = \begin{bmatrix} \dot{q} \\ D^{-1}(q)\big(-C(q,\dot{q}) - G(q)\big) \end{bmatrix},$$

$$g(x) = \begin{bmatrix} 0 \\ D^{-1}(q)B \end{bmatrix} \quad \text{and} \quad d(x_-) = \begin{bmatrix} q_- \\ \Delta(q_-)\dot{q}_- \end{bmatrix},$$

where $x = [q^\top \quad \dot{q}^\top]^\top \in \mathcal{X} = TQ = \mathbb{T}^N \times \mathbb{R}^N$, $q = [\varphi \quad \theta^\top]^\top = [\varphi \quad \theta_2 \quad \cdots \quad \theta_N] \in Q = \mathbb{T}^N$ is the N-dimensional toroidal manifold, $D \in \mathbb{R}^{N\times N}$ is the symmetrical positive definite inertia matrix, $C\dot{q} \in \mathbb{R}^N$ is the vector containing Coriolis and centrifugal terms, $G \in \mathbb{R}^N$ is the gravity vector, $B \in \mathbb{R}^{N\times N-1}$ is the input matrix and $u \in \mathcal{U}$ is the input vector, with $\mathcal{U}$ the set of admissible inputs. The impact map is given by $\Delta : \mathcal{S} \to \mathcal{X}$ which gives the state after impact $x_+(t) = \lim_{\tau \searrow t}(x(\tau))$ when the state just before impact $x_-(t) = \lim_{\tau \nearrow t}(x(\tau))$ enters the set $\mathcal{S} = \{x \in \mathcal{X} \mid \kappa(x) = 0\}$, with $\kappa : \mathcal{X} \to \mathbb{R}$ the impact detection function, which represents the distance between the tip of the swing foot and the ground. The $_-$ and $_+$ subscripts indicate the values of the variable just before and after the impact, respectively.

The equations of motion (1a) follow from the classical Euler-Lagrange method [22], whereas the impact map (1b) is derived as in [10] pp. 55-57, based on conservation of momentum [21]:

$$D_e\dot{q}_{e+} - D_e\dot{q}_{e-} = F, \tag{2}$$

with

$$F = J_p^\top F_r \quad \text{and} \quad J_p = \frac{\partial}{\partial q_e} p(q_{e-}).$$

Here $q_e = [x_s \quad y_s \quad \varphi \quad \theta^\top]^\top \in \mathbb{R}^2 \times \mathbb{T}^N$ is the extended state vector for the system not pin-pointed to the ground, $D_e \in \mathbb{R}^{N+2\times N+2}$ is the extended inertia matrix, $p = [x_s \quad y_s]^\top$ is the position of the swing foot, and $F_r \in \mathbb{R}^2$ is the vector of reaction forces occurring at the moment of strike of the swing foot with the ground. In the right-hand side of this expression, the principle of virtual work is used to map the ground reaction forces to joint torques. This momentum equation (2) represents $N + 2$ equations with $N + 4$ unknowns: $\dot{q}_{e+}$ and F. Two additional constraints come from the no-slip and no-rebound assumption because this implies that the velocity of the swing foot tip must vanish during the impact:

$$J_p\dot{q}_{e+} = 0 \tag{3}$$

Solving (2) together with (3) for $\dot{q}_{e+}$ yields (1b).

2.2 Model Analysis

In this section we present a mathematical analysis of the equilibrium sets and stability properties of the model derived in Section 2.1. This analysis is required for the derivation of the foot placement indicator (FPI) algorithm in Section 3. The following analysis is performed on the model when it is actively controlled in a rigid posture. We use as controller u in (1) a simple PD joint set-point regulating controller:

$$u = -K_p e - K_d\dot{\theta}, \tag{4}$$

where $e = (\theta - \theta_B) \in \mathbb{T}^{N-1}$ is the error and $\theta_B \in \mathbb{T}^{N-1}$ are desired joint angles that define a certain rigid posture, $K_p = \mathrm{diag}(K_{p,2}, \ldots, K_{p,N})$ and $K_d = \mathrm{diag}(K_{d,2}, \ldots, K_{d,N})$ with $K_{p,i} > 0$ and $K_{d,i} > 0$ respectively the proportional and derivative gains of joint i.

In the entire analysis we restrict the system to practically feasible joint angles, angles for which all link masses and the swing foot distance to the ground are non-negative:

$$\mathcal{X}_f = \{x \in \mathcal{X} \mid \kappa(x) \geq 0, y_i \geq 0, i = 1, \ldots, N\}. \tag{5}$$

In this feasible state space, the system has two sets of equilibrium points: a single support and a double support set. For the analysis of these sets of equilibrium points, we denote the kinetic energy by:

$$K(x) = \tfrac{1}{2}\dot{q}^\top D(q)\dot{q} = \tfrac{1}{2}\Big((\dot{x}_1^2 + \dot{y}_1^2)m_1 + \cdots + (\dot{x}_n^2 + \dot{y}_n^2)m_n\Big)$$
$$+\tfrac{1}{2}\big(\dot{\psi}_1^2 I_1 + \cdots + \dot{\psi}_n^2 I_n\big), \tag{6}$$

where x_i, y_i and ψ_i are a function of q and $\dot{q}$ as defined in Figure 1. The potential energy is denoted by:

$$P(q) = g(y_1 m_1 + \cdots + y_n m_n), \tag{7}$$

where g is the gravitational constant. In the next section, we first define the single support equilibrium set and determine its stability, after which we define the double support equilibrium set and determine its stability. All analyses are local, so in the final section we derive the basins of attraction of these equilibrium sets, which turns out to be the key ingredient for the FPI algorithm.

2.2.1 Single support equilibrium set

The first equilibrium set contains the joint angles for which the biped has one foot on the ground. We refer to this set as the set of balanced configurations, where a balanced configuration is defined as:

Definition 1: Balanced configuration; *A balanced configuration is a configuration in which the centre of mass*

(CoM) of the entire biped lies exactly above its stance foot and all velocities are zero.

For system (1) the position of the CoM is:

$$r_{CoM}(x) = \frac{1}{M}\sum_{i=1}^{N} m_i p_i\,(x), \tag{8}$$

where M is the total mass of the robot and m_i is the mass of link i located at $p_i = [x_i \quad y_i]^\top$. So the set of balanced configurations for system (1) according to Definition 1 is:

$$\mathcal{B} = \{x \in \mathcal{X}_f \mid r_{CoM}(x) = [0 \quad h]^\top, K(x) = 0\}, \tag{9}$$

where $h \geq 0$ is the height of the CoM.

To analyse the local stability properties of the balanced configuration set, we linearize system (1) around the equilibrium point $x_{\mathcal{B}} = [q_{\mathcal{B}}^\top \quad 0]^\top \in \mathcal{B}$, $u_{\mathcal{B}}$:

$$\dot{z} = Az + Bv, \tag{10}$$

where $z = x - x_{\mathcal{B}}$, $v = u - u_{\mathcal{B}}$ and

$$A = \frac{\partial f(x)}{\partial x}\Big|_{x_{\mathcal{B}},u_{\mathcal{B}}} = \begin{bmatrix} \mathbb{O}_N & \mathbb{I}_N \\ F_q & \mathbb{O}_N \end{bmatrix}, B = \frac{\partial g(x)u}{\partial u}\Big|_{x_{\mathcal{B}},u_{\mathcal{B}}} = g(x), \tag{11}$$

with $\mathbb{O}_N$ and $\mathbb{I}_N$ the N-dimensional zero and identity matrix respectively and

$$F_q = \frac{\partial\left(D^{-1}(q)\left(-C(q,\dot{q})\dot{q} - G(q)\right)\right)}{\partial q}\Bigg|_{x_{\mathcal{B}},u_{\mathcal{B}}}.$$

This linearized system is unstable since $\mathrm{tr}(A) = 0$ and, hence, at least one eigenvalue is non-negative. This also means that system (1) is locally unstable around the equilibrium set $\mathcal{B}$.

2.2.2 Double support equilibrium set

The second equilibrium set contains the joint angles for which the biped is in double support. A double support configuration is defined as:

Definition 2: Double support configuration; *A double support configuration is a configuration in which both feet of the biped are in contact with the ground and all velocities are zero.*

So, mathematically this set is given by:

$$\mathcal{D} = \{x \in \mathcal{X}_f \mid \kappa(x) = 0, K(x) = 0\}. \tag{12}$$

To analyse the stability properties of this equilibrium set, consider the Lyapunov function for the extended model with extended state $x_e = [q_e^\top \quad \dot{q}_e^\top]^\top$:

$$V(x_e) = K(x_e) + P(x_e) + \frac{1}{2}e^\top K_p e - P_{\mathcal{D}},$$

$$= \frac{1}{2}\dot{q}_e^\top D_e \dot{q}_e + P(x_e) + \frac{1}{2}e^\top K_p e - P_{\mathcal{D}} \geq 0, \tag{13}$$

where $P_{\mathcal{D}} = P(x_{\mathcal{D}}) + \frac{1}{2}e_{\mathcal{D}}^\top K_p e_{\mathcal{D}}$ is a constant offset in the potential energy datum, representing the potential energy in the double support equilibrium set, with $x_{\mathcal{D}}$ the state and $e_{\mathcal{D}}$ the tracking error of the desired rigid posture in the double support equilibrium set. The derivative is:

$$\begin{aligned}\dot{V}(x_e) &= \dot{q}_e^\top D_e \ddot{q}_e + \frac{1}{2}\dot{q}_e^\top \dot{D}_e \dot{q}_e + \dot{q}_e^\top \frac{\partial P_e}{\partial q_e} + \dot{\theta}^\top K_p e, \\ &= \dot{q}_e^\top\left(B_e u - G_e + \frac{\partial P_e}{\partial q_e}\right) + \frac{1}{2}\dot{q}_e^\top\left(\dot{D}_e - 2C_e\right)\dot{q}_e + \dot{\theta}^\top K_p e, \\ &= \dot{q}_e^\top B_e\left(-K_p e - K_d\dot{\theta}\right) + \dot{\theta}^\top K_p e, \\ &= -\dot{\theta}^\top K_d \dot{\theta} \leq 0,\end{aligned}$$

since $G_e = \frac{\partial P_e}{\partial q_e}$ and $\dot{D}_e - 2C_e$ is skew-symmetric. This time derivative shows that V is decreasing in the continuous part of the system (1a) as long as $\dot{\theta}$ is nonzero. As $\dot{\theta}$ may vanish while $\dot{\varphi}$ is nonzero, this derivative does not guarantee that V goes to zero. However, at the impacts, we have the transition (1b) for which the change in energy $E_i = V_+ - V_-$ is:

$$\begin{aligned}E_i &= K_+ + P_+ + \frac{1}{2}e_+^\top K_p e_+ - P_{\mathcal{D}} - K_- - P_- - \frac{1}{2}e_-^\top K_p e_- + P_{\mathcal{D}}, \\ &= \frac{1}{2}(\dot{q}_{e+}^\top D_e \dot{q}_{e+} - \dot{q}_{e-}^\top D_e \dot{q}_{e-}), \\ &= \frac{1}{2}\left(\dot{q}_{e+}^\top D_e \dot{q}_{e+} - (\dot{q}_{e+}^\top - F^\top D_e^{-1})D_e(\dot{q}_{e+} - D_e^{-1}F)\right), \\ &= \frac{1}{2}\left(\dot{q}_{e+}^\top J_p^\top F_r + F_r^\top J_p \dot{q}_{e+} - F^\top D_e^{-1}F\right), \\ &= -\frac{1}{2}F^\top D_e^{-1}F \leq 0,\end{aligned}$$

since D_e is a symmetric positive definite matrix, (2) and (3) are used to find expressions for $\dot{q}_{e-}$. Thus V is strictly decreasing in the continuous part of the system as well as at the impacts, which implies that V goes to zero such that the double support equilibrium set is locally asymptotically stable. In the next section we determine the basin of attraction of this equilibrium set to find out how local the result is.

2.2.3 Basin of attraction of double support equilibrium set

The next step is to determine the exact boundaries of the local stability of the double support equilibrium set. We can find these boundaries by excitation of the system from the double support equilibrium set. Again, we consider the system actively controlled in a desired fixed configuration $\theta_{\mathcal{B}}$. We try to establish a maximal bound on the excitation energy for the system being excited from the double support equilibrium set. So first, we analyse the maximal potential energy as follows:

Lemma 1: Maximal potential energy; *The potential energy in the balanced configuration $P_{\mathcal{B}}$ is the maximal potential energy in the absolute orientation φ for any fixed internal configuration $\theta_{\mathcal{B}}$.*

Proof. Let $\theta_{\mathcal{B}}$ be a fixed internal configuration, then using (8) there exists a unique $\varphi_{\mathcal{B}}$ that suffices:

$$r_{CoM,x} = 0, \tag{14}$$

where $r_{CoM,x}$ is the horizontal component of the CoM position. Moreover, let the potential energy for the fixed internal configuration $\theta_{\mathcal{B}}$ be given by $P(\varphi, \theta_{\mathcal{B}})$, then

$$\text{argmax}_{\varphi}\big(P(\varphi, \theta_{\mathcal{B}})\big) = \varphi_{\mathcal{B}}, \tag{15}$$

since the maximum is given by:

$$\frac{\partial P(\varphi, \theta_{\mathcal{B}})}{\partial \varphi} = 2Mr_{CoM,x} = 0, \tag{16}$$

which equals (14) and hence, the only solution is $\varphi_{\mathcal{B}}$.

What is interesting about Lemma 1 is that the potential energy in the unstable balanced equilibrium set is maximal. The excitation energy required to go from the double support equilibrium to the balanced configuration equilibrium in a fixed internal posture is thus the difference between the potential energies in these equilibriums:

$$P_{\mathcal{B}} - P_{\mathcal{D}} = K_{\mathcal{E}}, \tag{17}$$

where $P_{\mathcal{D}}$ is the potential energy in the double support equilibrium, $P_{\mathcal{B}}$ is the energy in the balanced configuration equilibrium and $K_{\mathcal{E}}$ is the excitation energy to bring the system from $\mathcal{D}$ to $\mathcal{B}$. The balanced configuration equilibrium set is unstable, so from this point the system might move further away from the double support equilibrium set. Thus, this point does not belong to the basin of attraction of the double support equilibrium set, and hence the maximal excitation energy for the double support equilibrium set is $K_{\mathcal{E}}$.

2.2.4 Balance of planar bipedal robots

We can use this fact to define balance in bipedal walking: when the robot makes a step, its configuration lies in the double support equilibrium set. If the robot locks its joints after impact and the kinetic energy is less than $K_{\mathcal{E}}$, the biped is not able to escape the basin of attraction of the double support equilibrium set and eventually stops in the stable double support configuration. So the step location is crucially important for the balance of bipedal robots, which is summarized in the following definition:

Definition 3: Balanced biped; *A biped is in balance as long as there exists a position to place its swing foot such that after the impact the total energy in the system is maximally the balanced configuration potential energy and no additional energy is added to the system.*

3. Foot Placement Indicator

In the previous analysis, the balance of planar bipedal robots has been addressed. In this section we show how proper foot placement can be used to keep the biped in balance. The previous section analysed the system properties after impact; the goal of this section is to find the step location before impact that results in balance after impact. First, we explain the general concept of the capture point (CP), foot placement estimator (FPE) and FPI algorithm, then show the differences and describe our motivation for developing the FPI algorithm, which is derived in the second part of this section.

The FPI algorithm is an extension of the FPE algorithm, which in turn is similar to the CP algorithm. The main concept behind these algorithms is practically equivalent. They are all based on energy conservation during a step. The difference between the algorithms lies in the models used to compute the proper foot placement location. The CP algorithm uses a linear inverted pendulum model [1, 17, 18] without impact dynamics, the FPE algorithm uses a planar inverted pendulum model with impact dynamics [6] and the FPI algorithm uses a planar model with distributed masses and impact dynamics [20].

The general concept behind these algorithms can be explained as follows. We try to find a point on the floor where the biped has to step and fix its internal posture such that, when its CoM moves precisely above its stance foot, all its energy has been converted into potential energy solely. Depending on the model used, this point corresponds to the CP, FPE or FPI. In the following explanation we use a full planar model and refer to this point as FPI, but the main idea also holds for the CP and FPE on a (linear) inverted pendulum model.

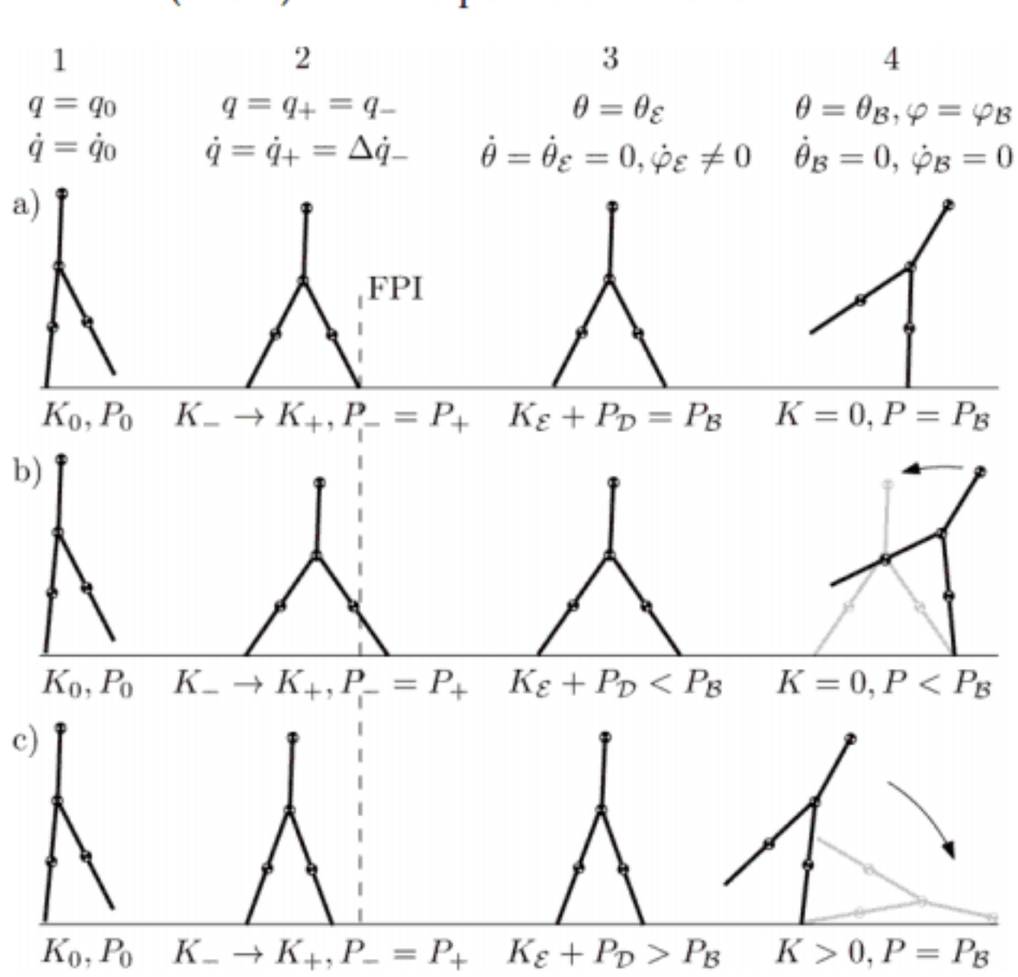

Figure 2. A schematic biped stepping relative to the FPI. a) Stepping precisely at the FPI will perfectly balance the CoM above the stance foot. b) Stepping after the FPI causes the biped to fall back onto the swing leg. c) Stepping before the FPI results in falling forward.

The FPI is visualized in Figure 2, where K denotes the kinetic energy, P the potential energy and q the state of

the system, containing the absolute orientation φ and joint angles θ. We can distinguish three possible scenarios for stepping near the FPI point: a) stepping onto the FPI point, b) stepping after the FPI point, and c) stepping before the FPI point. Each scenario consists of four different biped configurations: 1) the initial configuration, 2) the impact configuration, 3) the configuration in which the angular velocity in the actuated joints vanishes and the fixed posture is reached, and 4) the final configuration.

In each scenario the biped starts with the initial configuration q_0, velocity $\dot{q}_0$, kinetic energy K_0 and potential energy P_0. Then, the biped makes a step until an impact occurs when the swing foot hits the ground. The pre-impact configuration q_-, velocity $\dot{q}_-$ and energies K_- and P_- are mapped onto the post-impact configuration q_+, velocity $\dot{q}_+$ and energies K_+ and P_+ according to a rigid impact model. Some time after the impact, the angular velocity in the actuated joints vanishes and the actuated joint angles θ stop in the fixed posture $\theta_{\mathcal{E}} = \theta_{\mathcal{B}}$, whereas the absolute angle φ continues to vary. From this moment on, the total amount of energy in the system remains constant, but its exact value depends on where the biped stepped at the impact. Three different scenarios can occur (see Figure 2).

a. In situation 3 the biped steps precisely onto the FPI point and all the kinetic energy $K_{\mathcal{E}}$ is exactly converted into potential energy when the CoM moves above the stance foot. Thus, in situation 4 the biped comes to equilibrium in this balanced configuration with potential energy $P_{\mathcal{B}}$.
b. In situation 3 the biped stepped after the FPI point and all the kinetic energy $K_{\mathcal{E}}$ is converted into potential energy before the CoM moves above the stance foot. Thus, in situation 4 the biped never reaches the balanced configuration and falls back.
c. In situation 3 the biped steps before the FPI point and some kinetic energy $K_{\mathcal{E}}$ remains when the CoM moves above the stance foot. So, in situation 4 the biped reaches the balanced configuration with non-zero velocity and falls forward.

In [6, 17, 18], the model for computation of the FPE and CP consists of only one point mass on a (linear) inverted pendulum. It is arguable whether applying this model to a real complex biped with non-massless legs, torso and arms produces desired results [10], for three reasons [26]:

1. The total energy of the robot is not dependent on the configuration of the legs. So by moving the legs, the position of the FPE does not change. In bipeds with leg mass, the FPE position changes as the legs move.
2. The angular momentum of the biped is not influenced by its legs. During the impact of the swing leg with the ground, angular momentum is conserved. Thus, in bipeds with massless legs, the impact dynamics is extremely simplified over bipeds with leg mass.
3. There is only one possible balanced configuration. In bipeds with leg mass, there exist an infinite number of balanced configurations.

In the next section we present the FPI. This algorithm is a generalization of the FPE for planar bipeds with point feet and an arbitrary number of non-massless links on horizontal and flat ground.

3.1 FPI Algorithm

In the derivation of the FPI, we first consider the phase from the impact to the balanced bipedal position, after which we explain how this can be used to compute the FPI before the impact. The symbols $_{\mathcal{E}}$ and $_{\mathcal{B}}$ are used for the corresponding variable at the time instant when the relative angular joint velocities vanish and at the balanced configuration, respectively. Friction is neglected: as can be seen in Figures 2 scenario 3a), the energies in these distinct time instances are related through conservation of energy in the energy balance (17):

$$K(q_{\mathcal{E}}, \dot{q}_{\mathcal{E}}) + P(q_{\mathcal{D}}) = P(q_{\mathcal{B}}), \tag{18}$$

where $q_{\mathcal{E}} = [\varphi_{\mathcal{E}} \quad \theta_{\mathcal{E}}^{\top}]^{\top}$ is the state of the system at the moment the relative angular joint velocities vanish:

$$\dot{q}_{\mathcal{E}} = [\dot{\varphi}_{\mathcal{E}} \quad \dot{\theta}_{\mathcal{E}}^{\top}]^{\top} = [\dot{\varphi}_{\mathcal{E}} \quad 0]^{\top}. \tag{19}$$

We will now derive expressions for these angles and angular velocities as function of states before the impact, such that we can estimate the post-impact kinetic and potential energies and find the desired step location before the impact.

First we consider the actuated joint angles and angular velocities. These joints are actively controlled, so we can use feedback control to move them to a desired orientation. Here, we assume that we do not have to change the internal configuration of the biped after the impact. This orientation is fixed by feedback control throughout the rest of the step:

$$\theta_- = \theta_+ = \theta_{\mathcal{E}} = \theta_{\mathcal{B}}, \tag{20}$$

where $\theta_{\mathcal{B}}$ are the actuated joint angles at the balanced configuration. Thus, after the impact, we only have to bring the post-impact internal angular velocity $\dot{\theta}_+$ to zero using feedback control. What remains to be derived in (18) is the non-actuated angle $\varphi_{\mathcal{E}}$ and angular velocity $\dot{\varphi}_{\mathcal{E}}$. This joint is not actuated, so we cannot control it actively. We need to estimate the influence of the feedback control of the actuated joints on the non-actuated joint. This influence is estimated using conservation of angular momentum assuming that

feedback control can bring the actuated joint angular velocities to zero significantly fast, so that the change in the absolute angle can be neglected:

$$\varphi_{\mathcal{E}} = \varphi_{+} = \varphi_{-}. \tag{21}$$

Conservation of angular momentum now states that the time derivative of the angular momentum about a fixed point is equal to the moments induced by external forces acting about this fixed point ([21], p. 490). If we take the base coordinate frame as the fixed point, the only external force is gravity. We assumed that the configuration does not change, so gravitational forces do not change and we conserve angular momentum. Thus, we can use (2) and (3) with additional constraints induced by the feedback control on the internal configuration $p = [x_s \quad y_s \quad \theta_{-}^{\mathsf{T}}]^{\mathsf{T}}$ to find an expression for the non-actuated angular velocity:

$$\dot{\varphi}_{\mathcal{E}} = \Delta_{FPI}(q_{-})\dot{q}_{-}. \tag{22}$$

Now, by substituting (19), (20), (21) and (22) into (18) we obtain an expression in terms of states before the impact which has to be fulfilled to let the biped evolve to the balanced configuration:

$$K(\varphi_{-}, \theta_{-}, \Delta_{FPI}(\varphi_{-}, \theta_{-})\dot{q}_{-}, 0) + P(\varphi_{-}, \theta_{-}) = P(\varphi_{\mathcal{B}}, \theta_{-}). \tag{23}$$

This expression tells us that if the impact occurs and the configuration is $[\varphi_{-} \quad \theta_{-}^{\mathsf{T}}]^{\mathsf{T}}$, then the system will evolve to the configuration $[\varphi_{\mathcal{B}} \quad \theta_{-}^{\mathsf{T}}]^{\mathsf{T}}$ and, hence, the biped is balanced, because $[\varphi_{\mathcal{B}} \quad \theta_{-}^{\mathsf{T}}]^{\mathsf{T}} = [\varphi_{\mathcal{B}} \quad \theta_{\mathcal{B}}^{\mathsf{T}}]^{\mathsf{T}} \in \mathcal{B}$. Consequently, at every time instant before the impact, we solve this equation for φ_{FPI} and θ_{FPI} with current $\dot{q}$:

$$K(\varphi_{FPI}, \theta_{FPI}, \Delta_{FPI}(\varphi_{FPI}, \theta_{FPI})\dot{q}_{-}, 0)$$
$$+P(\varphi_{FPI}, \theta_{FPI}) = P(\varphi_{\mathcal{B}}, \theta_{FPI}). \tag{24}$$

Solving this equation for φ_{FPI} and θ_{FPI} gives us the desired FPI location that indicates in which configuration the foot needs to be placed to balance the biped [6].

The solution of (24) is in general not unique if the planar biped has more than two degrees of freedom. Here, there might be more pre-impact configurations such that the biped evolves to a balanced configuration. Multiple options exist to find a unique solution for bipeds with more degrees of freedom. The most elegant method is to use virtual holonomic constraints [10] to relate the actuated joints to the unactuated joint. In essence, one constrains the motion of the high order model to a lower order one, still taking into account the kinetic and potential energies of all links in the system. Alternatively, one could use a constraint optimization method which minimizes an objective function with (24) as constraint.

3.2 Foot Placement Controller

The FPI algorithm explained in the previous section can be cast into a controller that drives the system to the FPI configuration such that it properly places its foot and remains balanced. In short, the controller should solve (24) at each time instant before the impact as follows:

1. find an expression for $\varphi_{\mathcal{B}}$ as function of θ_{FPI} as in (15),
2. insert $\varphi_{\mathcal{B}}$ and θ_{FPI} in (7) to find the potential energy of the balanced configuration $P(\varphi_{\mathcal{B}}, \theta_{FPI})$,
3. assume that the impact occurs at the next time instant, so compute using (22) the absolute angular velocity of the biped $\dot{\varphi}_{\mathcal{E}} = \Delta_{FPI}(\varphi_{FPI}, \theta_{FPI})\dot{q}$ after the impact and after the relative angular joint velocities vanish,
4. use $\dot{\varphi}_{\mathcal{E}}$, φ_{FPI} and θ_{FPI} in (6) to compute the kinetic energy after the impact: $K(\varphi_{FPI}, \theta_{FPI}, \dot{\varphi}_{\mathcal{E}}, 0)$,
5. use φ_{FPI} and θ_{FPI} in (7) to compute the potential energy after the impact: $P(\varphi_{FPI}, \theta_{FPI})$,
6. solve the FPI equation (24) for φ_{FPI} and θ_{FPI}.

This desired configuration θ_{FPI} can be tracked as virtual holonomic constraint of φ by a controller so that if impact occurs and $\varphi = \varphi_{FPI}$, the foot is properly placed. Next, the practical implementation of such a controller is described.

We use the controller (4) as presented in Section 2.2. The desired joint angles $\theta_{\mathcal{B}}$ are now given accordingly:

$$\theta_{\mathcal{B}} = \begin{bmatrix} \theta_{\mathcal{B},st} \\ \hline \theta_{\mathcal{B},sw} \end{bmatrix} = \begin{bmatrix} 0 \\ -\varphi \\ \hline h(\varphi, \varphi_{FPI}, \theta_{FPI,sw}) \end{bmatrix}, \tag{25}$$

where the upper and lower part represent the stance and swing leg, respectively. The stance leg is kept straight, so all joint angles, except the hip, are controlled to remain zero. The hip joint controls the torso of the robot to remain perpendicular to the ground. The swing leg consists of virtual constraint functions that bring it from its initial configuration $\theta_{0,sw}$ to the desired FPI step orientation $\theta_{FPI,sw}$ as function of the absolute orientation φ. The virtual constraint has been chosen such that the swing leg velocity is zero at the initial absolute orientation φ_0 and at the desired FPI orientation φ_{FPI}:

$$h(\varphi, \varphi_{FPI}, \theta_{FPI,sw}) = \theta_{FPI,sw}$$
$$+(\theta_{0,sw} - \theta_{FPI,sw})\frac{(\varphi-\varphi_{FPI})^2}{(\varphi_0-\varphi_{FPI})^2}. \tag{26}$$

The desired FPI step $q_{FPI} = [\varphi_{FPI} \quad \theta_{FPI,st}^{\mathsf{T}} \quad \theta_{FPI,sw}^{\mathsf{T}}]^{\mathsf{T}}$, with $\theta_{FPI,st}$ and $\theta_{FPI,sw}$ respectively the stance and swing leg joint angles, is given by (24):

$$q_{FPI} = \text{argmin}_{\hat{q}_{-}}\left(\left(\hat{P}_{-} + \hat{K}_{-} - \hat{P}_{\mathcal{B}}\right)^2\right), \tag{27}$$

with the energy functions $\hat{P}_{-} := P(\hat{q}_{-})$, $\hat{P}_{\mathcal{B}} := P(\hat{q}_{\mathcal{B}})$ and $\hat{K}_{-} := K(\hat{q}_{-}, \Delta_{FPI}(\hat{q}_{-})\dot{q}_{-})$. Herein, $\hat{q}_{-}$ is the desired fixed posture that initiates impact. To simplify the optimization

and to find a unique global minimum we constrain these states to Cartesian positions on the ground:

$$\hat{q}_- = \begin{bmatrix} \hat{\varphi}_- \\ \hat{\theta}_- \end{bmatrix} = f_{IK}(x_{FPI}), \tag{28}$$

where f_{IK} is an inverse kinematics function and x_{FPI} is the Cartesian position along the ground. The inverse kinematics function f_{IK} is robot specific. It may be an analytical expression or a numerical optimization [24]. The balanced configuration state $\hat{q}_B$ can be computed from the balanced equilibrium configuration (15):

$$\hat{q}_B = \begin{bmatrix} \text{argmax}_{\varphi_B}\left(P(\hat{\varphi}_B, \hat{\theta}_-)\right) \\ \hat{\theta}_- \end{bmatrix}. \tag{29}$$

4. Simulation Example: Five-link Planar Biped

In this section, the FPI algorithm is applied to a model of a five-link biped. This model is shown in Figure 3. The model consists of five point masses and contains two lower legs, two upper legs and a torso. We derive the equations of motion as in (1) and implement these in a numerical simulation.

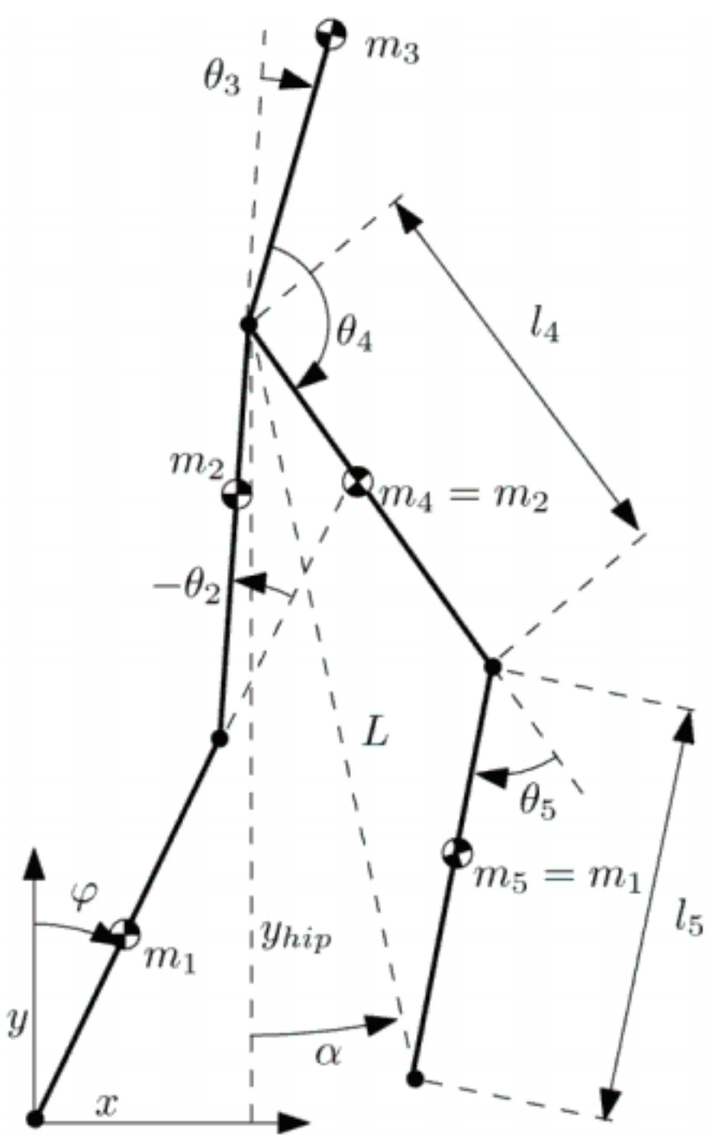

Figure 3. Schematic of the five-link planar biped model

We can now use the energy expressions (6) and (7) to solve the FPI equation (24) and use this in the feedback controller (4). As we have seen, there is no unique configuration from which the biped evolves to the balanced configuration, so we enforce the stance leg to be always fully stretched, $\theta_{FPI,2} = 0$, and the torso to be always perpendicular to the ground, $\theta_{FPI,3} = -\varphi$. Furthermore, we use a virtual holonomic constraint on the swing leg angles $\theta_{FPI,4}$ and $\theta_{FPI,5}$ in the parameter $\alpha = \varphi$, such that the swing leg is always as 'stretched' as possible, without penetrating the ground:

$$L = \min\left(l_4 + l_5, \frac{y_{hip} - L_{fc}(\alpha)}{\cos(\alpha)}\right), \tag{30}$$

where $L_{fc} \geq 0$ is a desired foot clearance height. In the first part of the step this clearance height is kept constant. When the swing foot passes the vertical, i.e. $\alpha > 0$, the value is decreased to zero so that the biped completes the step with a fully stretched swing leg. Expression (30) for the virtual leg length L can be used in the inverse kinematics function (28) so that we can uniquely solve the FPI equation for α_{FPI} [24].

We performed three simulations. In each simulation, the robot starts with the same initial configuration and velocity. The FPI algorithm computes at each time instant before the impact the FPI angle α_{FPI} from (24). In two simulations we intentionally perturbed the desired FPI angle with a constant offset to show the differences between the three scenarios, as indicated in Figure 2. Joint PD feedback control brings the actual α to the (perturbed) FPI angle, as can be seen in the bottom plots in Figure 4. These figures show, from left to right, that the robot steps onto the FPI point, steps after the FPI point and steps before the FPI point. The dotted vertical lines indicate the moments of impact. In the top plots in Figure 4 relevant energies are shown. Here, the actual kinetic energy K, potential energy P and total energy E are plotted, as well as the estimated post-impact kinetic energy $K_\mathcal{E}$, post-impact potential energy $P_\mathcal{D}$ and final potential energy in the balanced configuration $P_\mathcal{B}$.

We can observe in each simulation that, before the impact, the biped falls forward. During this fall, the height of the CoM decreases and its velocity increases. This corresponds with the plots if we compare the initial energies with the energies just before the impact. The kinetic energy K slightly increases whereas the potential energy P decreases. At both moments the actuated joint velocities are almost zero, since the swing leg is in its initial and FPI configuration. The energies almost correspond to those of the CoM of the biped. Between the initial and impact moment, the swing leg is accelerated and decelerated, which causes the increase and decrease in kinetic energy.

At the impact, a clearly visible drop in kinetic energy can be noticed, whereas the potential energy is constant over the impact. This also results in a steep drop in the total energy E at the impact. After the impact, even more energy is dissipated when the relative angular joint velocities vanish (visible in the inset in the energy plots). After the relative angular joint velocities vanish, the total energy E in the system remains constant. The biped continues its motion forward and converts the kinetic energy into potential energy. The notable differences between the simulations can be explained as follows-

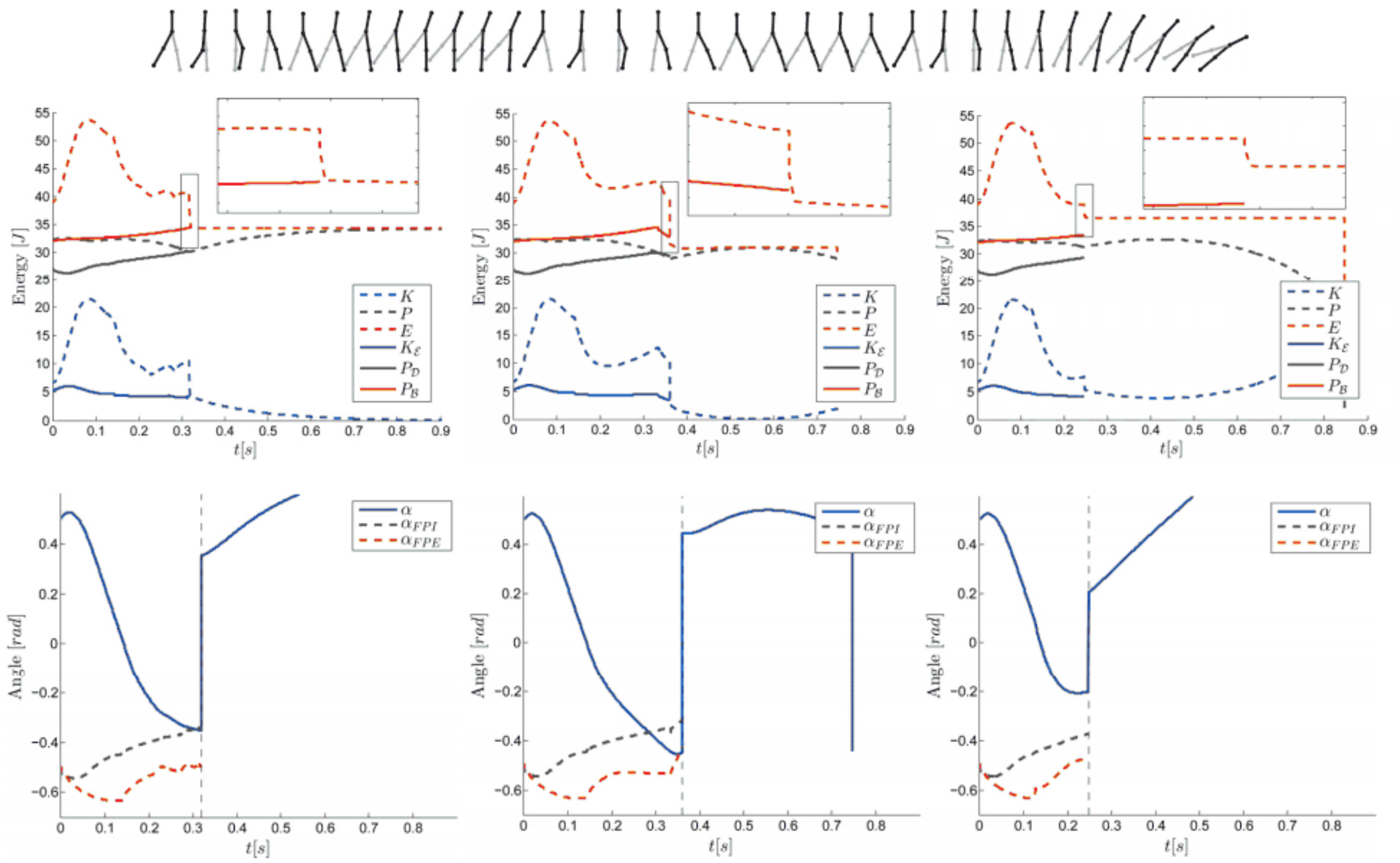

Figure 4. Simulation results for the three different scenarios. Top figures show relevant energies: actual kinetic energy K, actual potential energy P, actual total energy E, estimated post-impact kinetic energy $K_\mathcal{E}$, estimated post-impact potential energy $P_\mathcal{D}$ and estimated balanced configuration potential energy $P_\mathcal{B}$. The inset is a magnification of the marked area. Bottom figures show the swing leg actual angle α, desired FPI angle α_{FPI} and FPE angle α_{FPE}.

a. The FPI method accurately estimates the post-impact total energy, since the post-impact kinetic energy $K_\mathcal{E}$, post-impact potential energy $P_\mathcal{D}$ and balanced configuration potential energy $P_\mathcal{B}$ coincide with the actual kinetic energy K, potential energy P and total energy E after the impact. When the relative angular joint velocities vanish, the total energy in the system remains constant, so the relation $K_\mathcal{E} + P_\mathcal{D} = P_\mathcal{B}$ holds. Indeed, we can observe that the biped converts all the kinetic energy into potential energy and stops at the balanced configuration.
b. The FPI method underestimates the post-impact total energy. When the relative angular joint velocities vanish, the total energy remains constant, but is smaller than the required balanced configuration potential energy: $K_\mathcal{E} + P_\mathcal{D} < P_\mathcal{B}$. The biped converts all the kinetic energy into potential energy before it reaches the balanced configuration and falls back.
c. The FPI method overestimates the post-impact total energy. When the relative angular joint velocities vanish, the total energy remains constant, but is larger than the required balanced configuration potential energy: $K_\mathcal{E} + P_\mathcal{D} = P_\mathcal{B}$. The biped reaches the balanced configuration with non-zero kinetic energy and falls.

We also compute the original FPE angle α_{FPE} as in [6] during the simulations and compare these to α_{FPI} in the bottom plots of Figure 4. We can clearly see that the original FPE algorithm does not estimate the foot placement properly. We believe that this is caused by simplification of the five-link model to an inverted pendulum. The movement of the swing leg is large and it significantly influences the kinetic and potential energy of the biped.

This comparison can motivate the further development of the FPI method, such as to overcome some limitations of the method in its current form and make it applicable for walking and three-dimensional bipeds. The main problem of the current approach is the assumption that the relative joint velocities vanish significantly fast, such that the energy is conserved after the impact. This energy conservation is required to prove that the FPI controller guarantees balance, but limits its usability to the one-step case with fixed desired configuration, as discussed in this paper. We have obtained simulation results that show that continuously stepping before the FPI point results in walking on planar bipeds with point feet [25]; however, we were not able to mathematically prove the stability for this case. We expect that this problem can be solved by replacing the PD controller by an output regulation controller as presented in [10]. This controller attracts the full system dynamics (1) to a lower dimensional zero dynamics. This zero dynamics is Lagrangian by

definition, and in this way energy is conserved during a step. We expect that we can apply the FPI algorithm to zero dynamics and prove its stability when walking. Furthermore, we believe that we can extend this zero dynamics framework to the three-dimensional case and show stable bipedal manoeuvring. Moreover, since the dimension of the zero dynamics is lower than the full system model, the computations become easier and might be feasible on a physical system in real time.

5. Conclusion and Future Work

In this paper we introduced the foot placement indicator (FPI), which is an extension of the foot placement estimator method to planar bipeds with point feet and an arbitrary number of non-massless links on horizontal and flat ground. The FPI algorithm is derived by thorough mathematical analysis of the equilibrium sets and stability properties of these planar biped models. The algorithm can accurately compute where a biped needs to step in order to evolve to a balanced configuration, i.e., the configuration in which the biped is in equilibrium and its centre of mass lies exactly above its stance foot. We derived the necessary expressions used to calculate the FPI point. These expressions are based on energy conservation in the system, properly taking into account energy losses during the impact. We showed applicability of the algorithm in simulations of a five-link planar biped. The simulation results showed that the FPI algorithm works better than the FPE algorithm on robots with non-massless links. It can accurately compute the FPI point where the biped needs to step to evolve to the balanced configuration. Future work includes extension of the algorithm to walking and three-dimensional bipeds, which we expect to achieve via an output regulation controller.

6. References

[1] de Boer, T. (2012) Foot placement in robotic bipedal locomotion. Ph.D. thesis, Delft University of Technology.

[2] Pratt, J., Dilworth, P., and Pratt, G. (1997) Virtual model control of a bipedal walking robot. IEEE International Conference on Robotics and Automation, Albuquerque, USA, pp. 193-198.

[3] Spong, M. and Bullo, F. (2005) Controlled symmetries and passive walking. IEEE Transactions on Automatic Control, vol. 50, nr. 7, pp. 1025-1031.

[4] Kajita, S., Yamaura, T., and Kobayashi, A. (1992) Dynamic walking control of a biped robot along a potential energy conserving orbit. IEEE Transactions on Robotics and Automation, vol. 8, nr. 4, pp. 431-438.

[5] Pratt, J., Carff, J., Drakunov, S., and Goswami, A. (2006) Capture point: A step toward humanoid push recovery. 6th IEEE-RAS International Conference on Humanoid Robots, Genove, Italy, pp. 200-207.

[6] Wight, D., Kubica, E., and Wang, D.L. (2008) Introduction of the foot placement estimator: A dynamic measure of balance for bipedal robotics. Journal of Computational and Nonlinear Dynamics, vol. 3, nr. 1, pp. 1-9.

[7] Garcia, M., Chatterjee, A., Ruina, A., and Coleman, M. (1998) The simplest walking model: Stability, complexity, and scaling. Journal of Biomechanical Engineering, vol. 120, nr. 2, pp. 281-288.

[8] McGeer, T. (1990) Passive dynamic walking. The International Journal of Robotics Research, vol. 9, nr. 2, pp. 62-82.

[9] Wisse, M., Schwab, A., van der Linde, R., van der Helm, F. (2005) How to keep from falling forward: elementary swing leg action for passive dynamic walkers. IEEE Transactions on Robotics, vol. 21, nr. 3, pp. 393-401.

[10] Westervelt, E., Grizzle, J., Chevallereau, C., Choi, J., and Morris, B. (2007) Feedback control of dynamic bipedal robot locomotion. New York: CRC Press.

[11] Kajita, S., Kanehiro, F., Kaneko, K., Fujiwara, K., Harada, K., Yokoi, K., Hirukawa, H. (2003) Resolved momentum control: Humanoid motion planning based on the linear and angular momentum. IEEE/RSJ International Conference on Intelligent Robots and Systems, Las Vegas, USA, pp. 1644-1650.

[12] Goswami, A. and Kallem, V. (2004) Rate of change of angular momentum and balance maintenance of biped robots. IEEE International Conference on Robotics and Automation, Barcelona, Spain, pp. 3785-3790.

[13] Vukobratović, M. and Borovac, B. (2004) Zero-moment point-thirty five years of its life. International Journal of Humanoid Robotics, vol. 25, nr. 9, pp. 157-173.

[14] Goswami, A. (1999) Foot rotation indicator (FRI) point: A new gait planning tool to evaluate postural stability of biped robots. IEEE International Conference on Robotics and Automation, Detroit, USA, pp. 47-52.

[15] Stephens, B. (2007) Humanoid push recovery. 7th IEEE-RAS International Conference on Humanoid Robots, Pittsburg, USA, pp. 589-595.

[16] Popovic, M., Goswami, A., and Herr, H. (2005) Ground reference points in legged locomotion: Definitions, biological trajectories and control implications. International Journal of Robotics Research, vol. 24, nr. 12, pp. 1013-1032.

[17] Koolen, T., de Boer, T., Rebula, J., Goswami, A., and Pratt, J. (2012) Capturability-based analysis and control of legged locomotion, part 1: Theory and application to three simple gait models. International Journal of Robotics Research, vol. 31, nr. 9 pp. 1094-1113.

[18] Pratt, J., Koolen, T., de Boer, T., Rebula, J., Cotton, S., Carff, J., Johnson, M., and Neuhaus, P. (2012) Capturability-based analysis and control of legged locomotion, part 2: Application to m2v2, a lower

body humanoid. International Journal of Robotics Research, vol. 31, nr. 10, pp. 1117-1133.

[19] van Zutven, P., Kostić, D., and Nijmeijer, H. (2010) On the stability of bipedal walking. LNAI series: Simulation, Modeling, and Programming for Autonomous Robots, Darmstadt, Germany, pp. 521-532.

[20] van Zutven, P., Kostić, D., and Nijmeijer, H. (2012) Foot placement for planar bipeds with point feet. IEEE International Conference on Robotics and Automation, Saint Paul, USA, pp. 983-988.

[21] Hurmuzlu, Y., Génot, F., and Brogliato, B. (2004) Modeling, stability and control of biped robots – a general framework. Automatica, vol. 40, nr. 10, pp. 1647-1664.

[22] Spong, M., Hutchinson, S., and Vidyasagar, M. (2006) Robot modeling and control. New York: John Wiley and Sons, Inc.

[23] Meriam, J., Kraige, L., and Palm, W. (1993) Engineering mechanics: dynamics, New York: John Wiley and Sons, Inc.

[24] Siciliano, B. and Sciavicco, L. and Villani, L. (2009) Robotics: modelling, planning and control. London: Springer Verlag.

[25] van Zutven, P.W.M. and Nijmeijer, H. (2012) Balance of humanoid robots by proper foot placement. 7th Annual Dynamic Walking Conference, Pensacola, USA, pp. 4-7

[26] Assman, T.M., van Zutven, P.W.M. and Nijmeijer, H. (2013) Qualitative validation of humanoid robot models through balance recovery side-stepping experiments. IEEE International Conference on Robotics and Automation, Karlsruhe, Germany.